Digital Pre-Equalization for OFDM-Based VLC Systems: Centralized or Distributed?

Chen Chen, *Member, IEEE*, Yungui Nie, Min Liu, Yufeng Du, Ruisi Liu, Zixian Wei, H. Y. Fu, *Senior Member, IEEE*, and Binbin Zhu

***Abstract*— We propose and experimentally demonstrate a distributed digital pre-equalization (DPE) technique for orthogonal frequency division multiplexing (OFDM)-based bandlimited visible light communication (VLC) systems. In the VLC system applying distributed DPE, the subcarriers are divided into two bands, where the bandwidth and the power of each band can be flexibly adjusted to maximize the achievable data rate of the system. Hence, distributed DPE exhibits much higher tolerance against light-emitting diode (LED) nonlinearity than conventional centralized DPE. Experimental results verify the superiority of distributed DPE for OFDM-based bandlimited VLC systems. More specifically, a data rate of 976.6 Mbit/s is achieved by using distributed DPE, which corresponds to an achievable rate improvement of 25% in comparison to centralized DPE.**

***Index Terms*— Visible light communication, orthogonal frequency division multiplexing, digital pre-equalization.**

I. Introduction

VISIBLE light communication (VLC) using light-emitting diodes (LEDs) has attracted extensive attention in recent years, owing to its merits such as abundant spectrum resources, high security and no electromagnetic interference [1]. Lately, VLC-enabled LiFi networks have revealed great potential for 6G and Internet of things applications [2], [3]. Nevertheless, one key challenge that must be faced to develop high-speed VLC systems is the limited modulation bandwidth of commercial white LEDs, which is typically about a few MHz [4]. So far, many techniques have been proposed for capacity improvement of bandlimited VLC systems, including blue filtering [5], pre-equalization [6], [7], orthogonal frequency division multiplexing (OFDM) with high-order quadrature amplitude modulation (QAM) constellations [8], multiple-input multiple-output (MIMO) transmission [9], non-orthogonal multiple access [10], [11], and so on. Among them, blue filtering and pre-equalization can directly extend the modulation bandwidth of LEDs. Although bandwidth extension can be obtained by blue filtering, the received signal power is inevitably decreased, leading to a reduced signal-to-noise ratio (SNR). In contrast, pre-equalization can efficiently extend LED bandwidth without sacrificing the received signal power, which has been widely applied in VLC systems. Moreover, as a capacity-approaching modulation technique, adaptive OFDM with bit and power loading has also been applied in high-speed VLC systems [12]. However, the application of adaptive OFDM with bit and power loading in practical VLC systems might be challenging due to its high implementation complexity and the need of instantaneous SNR feedback information. As a result, OFDM modulation with pre-equalization can be a promising candidate for practical low-complexity VLC systems.

Generally, pre-equalization techniques can be divided into two categories: one is analog pre-equalization (APE), and the other is digital pre-equalization (DPE). Specifically, APE is realized by using analog hardware circuits [6], [13], while DPE is performed via software digital signal processing (DSP) [7], [14]. Considering that LEDs might have different frequency responses, a specific pre-equalization circuit should be designed for each LED and hence APE is lack of flexibility. In contrast, the design of DPE is highly flexible through DSP which can be adaptively adjusted according to the specific frequency response of the LED. Although DPE can efficiently extend the modulation bandwidth of OFDM-based bandlimited VLC systems, it performs power compensation in a centralized manner. Considering that practical LEDs exhibit severe nonlinearity, the power penalty of such a centralized DPE scheme might be an issue in particular for constant illumination optical output from a nonlinear LED, due to the excessive amplification of the power of high-frequency subcarriers.

In this letter, we propose and experimentally demonstrate a novel distributed DPE technique for OFDM-based bandlimited VLC systems. By performing DPE in a distributed manner, the adverse effect of LED nonlinearity can be efficiently mitigated. Moreover, the distributed DPE can be further optimized according to the specific frequency response of the VLC system, so as to maximize the achievable data rate of the system.

II. Principle of Distributed DPE

To eliminate the power difference between low-frequency and high-frequency subcarriers in OFDM-based VLC system

Manuscript received June 21, 2021; revised July 23, 2021; accepted August 10, 2021. Date of publication August 13, 2021; date of current version August 19, 2021. This work was supported in part by the National Natural Science Foundation of China under Grant 61901065, in part by the Fundamental Research Funds for Central Universities under Grant 2021CDJQY-013, and in part by the China Postdoctoral Science Foundation under Grant 2021M693744. *(Corresponding author: Chen Chen.)*

Chen Chen, Yungui Nie, Min Liu, Yufeng Du, and Ruisi Liu are with the School of Microelectronics and Communication Engineering, Chongqing University, Chongqing 400044, China (e-mail: c.chen@cqu.edu.cn).

Zixian Wei and H. Y. Fu are with Tsinghua–Berkeley Shenzhen Institute (TBSI), Tsinghua University, Shenzhen 518055, China.

Binbin Zhu is with Shenzhen Hua Chuang Chip Lighting Company, Ltd., Shenzhen 518027, China.

Color versions of one or more figures in this letter are available at https://doi.org/10.1109/LPT.2021.3104618.

Digital Object Identifier 10.1109/LPT.2021.3104618

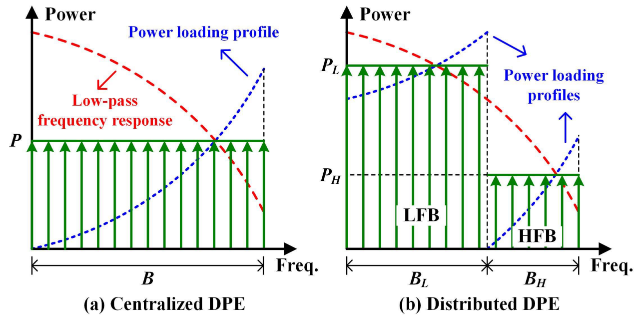

Fig. 1. Illustration of the received OFDM spectra with (a) centralized DPE and (b) the proposed distributed DPE.

with a low-pass frequency response, centralized DPE was proposed which allocates more power to the subcarriers in the high-frequency region so that all the subcarriers can have a comparable power [7]. To implement centralized DPE, a power loading profile is first calculated according to the measured low-pass frequency response of the VLC system. Then, the obtained power loading coefficients are multiplied with the corresponding input data of the subcarriers before executing the inverse fast Fourier transform (IFFT). Fig. 1(a) depicts the spectrum of the received OFDM signal with centralized DPE. It can be found that the received power of all the subcarriers is comparable after performing centralized DPE, and thus the OFDM signal can have flat SNR and bit error rate (BER) profiles. Although centralized DPE can compensate the high-frequency attenuation, the received power of low-frequency subcarriers is greatly reduced after power re-allocation. Hence, centralized DPE might overcompensate the power attenuation of the subcarriers in the high-frequency region, which leads to significant power loss for the subcarriers in the low-frequency region. Furthermore, since high-frequency subcarriers might be allocated with an excessively high power with centralized DPE, they become much more vulnerable to LED nonlinearity. Therefore, more power dose not necessarily bring lower BER in OFDM-based VLC systems employing centralized DPE.

Considering the issues of centralized DPE, we for the first time propose a novel distributed DPE technique for OFDM-based bandlimited VLC systems. The proposed distributed DPE can be considered as the combination of centralized DPE and adaptive bit/power loading, where the centralized DPE is performed with respect to two different bands and the adaptive bit/power loading is applied for the two equalized bands. The basic principle of distributed DPE is illustrated in Fig. 1(b), where the power of the subcarriers is compensated in a distributed manner. Specifically, the subcarriers within the signal bandwidth B are divided into two bands, i.e., the low-frequency band (LFB) and the high-frequency band (HFB). The bandwidths of the LFB and the HFB are respectively denoted by B_L and B_H, and we have $B_L + B_H = B$. It should be noted that the subcarriers within the signal bandwidth can also be divided into more than two bands when performing distributed DPE, and the extreme case in dividing the signal bandwidth is that each subcarrier is treated as an individual band. In this case, distributed DPE becomes exactly the same as the well-known adaptive bit and power loading scheme, which exhibits high transceiver complexity. Therefore, in order to keep the transceiver complexity as low as possible, the subcarriers within the signal bandwidth is only divided into two bands in the proposed distributed DPE.

Differing from centralized DPE, the power compensation in distributed DPE is carried out for the LFB and the HFB individually. As shown in Fig. 1(b), two individual power loading profiles are calculated for the LFB and the HFB, respectively. Using the obtained power loading coefficients, the powers of the LFB and the HFB can be re-allocated accordingly. Owing to the distributed operation of DPE, the LFB and the HFB can be allocated with different powers. Letting P_L and P_H respectively represent the allocated powers to the LFB and the HFB, the total power of the LFB and the HFB always remains the same, i.e., $P_L + P_H = P_{\text{tot}}$ where P_{tot} denotes the total transmitted power. In the next, we define two key parameters for distributed DPE. The first parameter is the bandwidth allocation ratio α, which is defined as the ratio between the bandwidth of the LFB and the overall signal bandwidth, i.e.,

$$\alpha = \frac{B_L}{B} = \frac{B_L}{B_L + B_H}. \tag{1}$$

The second parameter is the power allocation ratio β, which can be defined as the ratio between the power of the HFB and the power of the LFB, i.e.,

$$\beta = \frac{P_H}{P_L}. \tag{2}$$

By applying uniform bit loading on per subcarrier in the LFB or the HFB, the achievable data rate of the OFDM-based VLC system adopting distributed DPE can be calculated by

$$R = \eta_L B_L + \eta_H B_H = [\alpha\eta_L + (1-\alpha)\eta_H]B, \tag{3}$$

where η_L and η_H denote the numbers of bits per unit bandwidth that can be transmitted by LFB and HFB, respectively.

III. Experimental Setup and Results

In this section, we conduct experiments to investigate the performance of distributed DPE in OFDM-based bandlimited VLC systems. Fig. 2 depicts the experimental setup, where the insets (a) and (b) show the schematics of OFDM modulation and demodulation with distributed DPE, respectively. For OFDM modulation, the serial input bits are separated into two parts via serial-to-parallel (S/P) conversion, where one part is mapped into QAM symbols for the LFB and the other part is mapped into QAM symbols for the HFB. Subsequently, distributed DPE is performed according to the measured low-pass frequency response. Before executing the IFFT, the Hermitian symmetry (HS) constraint is imposed so as to generate a real-valued output signal. After parallel-to-serial (P/S) conversion, the transmitted OFDM signal is obtained. For OFDM demodulation, time synchronization is first carried out and then the serial data are converted into the parallel data via S/P conversion. After performing FFT and frequency-domain equalization (FDE), the QAM symbols corresponding to the LFB and the HFB are respectively demapped, and the output bits are finally recovered via P/S conversion.

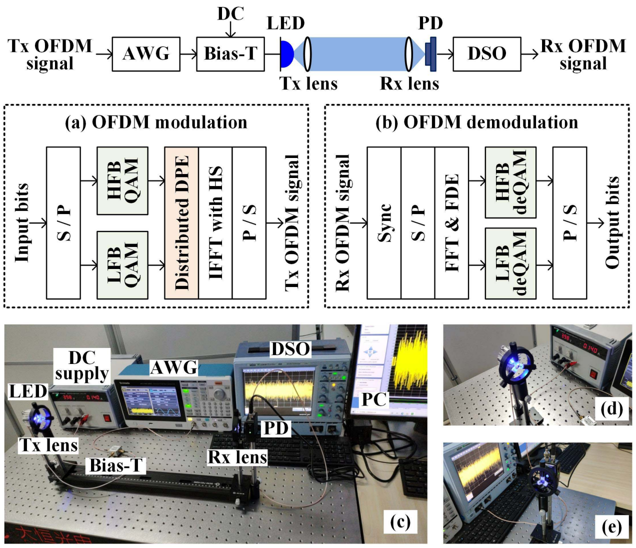

Fig. 2. Experimental setup of a point-to-point VLC system using a blue mini-LED. Insets: schematics of OFDM (a) modulation and (b) demodulation with distributed DPE, and photos of (c) the overall system, (d) the transmitter and (e) the receiver.

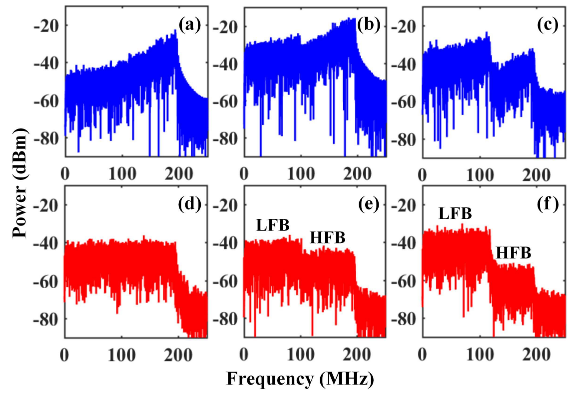

Fig. 3. Transmitted spectra of OFDM signals with (a) centralized DPE, (b) distributed DPE with $\alpha = 0.5$ and $\beta = 0.5$, and (c) distributed DPE with $\alpha = 0.6$ and $\beta = 0.1$, and received spectra of OFDM signals with (d) centralized DPE, (e) distributed DPE with $\alpha = 0.5$ and $\beta = 0.5$, and (f) distributed DPE with $\alpha = 0.6$ and $\beta = 0.1$.

The digital OFDM signal generated offline by MATLAB is loaded to an arbitrary waveform generator (AWG, Tektronix AFG31102) with a sampling rate of 500 MSa/s, where the length of the IFFT/FFT is 256 and a total of 100 subcarriers are used to carry valid QAM symbols. Hence, the bandwidth of the OFDM signal is 195.3 MHz. In order to obtain a non-negative signal, a 140-mA DC bias current is added via a bias-tee (Mini-Circuits, ZFBT-6GW+) and the resultant signal is used to drive a blue mini-LED (HCCLS2021CHI03). The corresponding -3dB bandwidth of the VLC system is 86 MHz. At the receiver side, a photodetector (PD, Thorlabs PDA10A2) with a bandwidth of 150 MHz and an active area of 0.8 mm^2 is adopted to detect the optical signal. The received signal is recorded by a digital storage oscilloscope (DSO, LeCroy WaveSurfer 432) with a sampling rate of 2 GSa/s, which is further demodulated offline. Moreover, to achieve a relatively high SNR, a pair of biconvex lenses each with a diameter of 12.7 mm and a focal length of 20 mm are used to align the blue mini-LED and the PD. In the experiments, the transmission distance is set to 60 cm. The photo of the overall system is shown in inset (c) of Fig. 2, while insets (d) and (e) show the photos of the transmitter and the receiver, respectively.

In the next, we compare the transmitted and received spectra of OFDM signals for three cases: (a) centralized DPE, (b) distributed DPE with $\alpha = 0.5$ and $\beta = 0.5$, and (c) distributed DPE with $\alpha = 0.6$ and $\beta = 0.1$. As shown in Figs. 3(a) and (e), the received OFDM signal has a flat spectrum when centralized DPE is applied. Although the spectrum becomes flat, the power of low-frequency subcarriers is substantially reduced. In contrast, when distributed DPE is adopted, the overall spectrum is divided into two parts, i.e., LFB and HFB. It can be found from Figs. 3(b), (f), (c) and (d) that distributed DPE can be flexibly performed by adjusting α and β.

We further investigate the received SNR for different cases by changing the peak-to-peak voltage (Vpp) of the OFDM signal. As shown in Fig. 4(a), for the case without DPE, the received SNR is generally increased with the increase of Vpp. However, for the case of centralized DPE, the received SNR is first increased and then reduced with the increase of Vpp, and the highest SNR of 18.1 dB is achieved when Vpp = 3 V. As we can observe, the received SNR with centralized DPE is higher than that without DPE only when the Vpp is relatively small. For a large Vpp of 5 V, the received SNR with centralized DPE is much lower than that without DPE, which is mainly due to the performance degradation of high-frequency subcarriers caused by the adverse effect of LED nonlinearity. For the case of distributed DPE with $\alpha = 0.5$ and $\beta = 0.5$, the LFB and the HFB have the same bandwidth, but the LFB achieves relatively higher SNRs than the HFB. For the case of distributed DPE with $\alpha = 0.6$ and $\beta = 0.1$, the SNR difference between the LFB and the HFB becomes much more significant, since the most portion of the transmitted power is allocated to the LFB. Based on the measured SNR performance of the LFB and the HFB, we can directly obtain the number of bits per unit bandwidth that can be transmitted by the LFB and the HFB. To perform bit loading and calculate the achievable rate, M-ary QAM constellations are considered and the BER threshold of 3.8×10^{-3} is adopted to yield the corresponding minimum SNR requirement.

In the proposed distributed DPE, the two parameters (i.e., α and β) can be flexibly adjusted. Hence, the performance of distributed DPE can be optimized by finding optimal α and β values, so as to maximize the achievable data rate of the VLC system. Fig. 4(b) shows the achievable rate versus both α and β for Vpp = 4 V, where α is in the range from 0.2 to 0.8 and β is in the range from 0.1 to 0.9. It can be clearly seen that there is one set of optimal α and β values, i.e., ($\alpha_{opt} = 0.5$, $\beta_{opt} = 0.5$), to achieve maximum data rate of 976.6 Mbit/s for Vpp = 4 V, as highlighted in the red star. The optimal α and β values might be different for different Vpp values.

Finally, Fig. 4(c) compares the maximum achievable rate versus Vpp for different cases. For the case without DPE, the achievable rate is gradually increased when Vpp is increased from 1 to 3 V, and it remains the same at 781.3 Mbit/s for a higher Vpp of 4 and 5 V. For the case

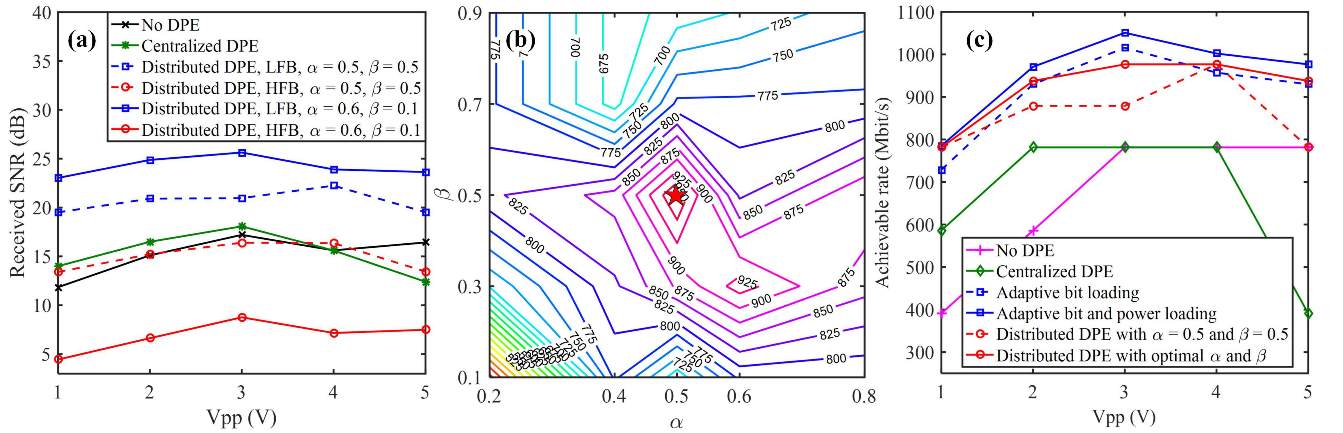

Fig. 4. Experimental results: (a) received SNR vs. Vpp, (b) achievable rate (Mbit/s) vs. both α and β for Vpp = 4 V, and (c) achievable rate vs. Vpp.

of centralized DPE, the achievable rate is firstly increased and then remains stable, and finally decreased with the increase of Vpp. Specifically, the achievable rate with centralized DPE is higher than that without DPE for a relatively small Vpp of 1 and 2 V, and the same data rate is achieved for a moderate Vpp of 3 and 4 V. For a high Vpp of 5 V, the achievable rate with centralized DPE is greatly lower than that without DPE, and this performance degradation is mainly caused by the adverse effect of LED nonlinearity on the performance of high-frequency subcarriers. In contrast, when distributed DPE with $\alpha = 0.5$ and $\beta = 0.5$ is employed, substantial achievable rate improvement can be obtained. As we can see, a maximum data rate of 976.6 Mbit/s is achieved for Vpp = 4 V, which indicates a 25% improvement of achievable rate by using distributed DPE with $\alpha = 0.5$ and $\beta = 0.5$ compared with that using centralized DPE. Moreover, the achievable rate utilizing distributed DPE can be further maximized by setting optimal α and β values. For example, the achievable rate is increased from 878.9 to 976.6 Mbit/s for Vpp = 3 V, when optimal α and β values are considered. It can be further observed that distributed DPE with optimal α and β achieves comparable performance as adaptive bit loading, while adaptive bit and power loading only performs slightly better than distributed DPE with optimal α and β. Therefore, dividing the bandwidth into three or more bands can only slightly increase the achievable rate of distributed DPE, but with substantially increased implementation complexity. In brief, the proposed distributed DPE can obtain greatly improved achievable rate in comparison to centralized DPE with only slightly increased complexity, while it achieves comparable rate in comparison to adaptive bit and power loading with much reduced complexity. Furthermore, the complexity of the proposed distributed DPE technique can be further reduced by adopting fixed bandwidth and power allocation ratios (i.e., $\alpha = 0.5$ and $\beta = 0.5$), which can also achieve satisfactory rate performance.

IV. Conclusion

In this letter, we have proposed and experimentally demonstrated a novel distributed DPE technique for OFDM-based bandlimited VLC systems with low transceiver complexity. In the proposed distributed DPE, the subcarriers are divided into two bands where the bandwidth and the power of each band can be flexibly adjusted and optimized. As a result, distributed DPE is more robust to LED nonlinearity than centralized DPE. The obtained experimental results show that distributed DPE can achieve substantially improved data rate than centralized DPE. Therefore, the proposed distributed DPE technique has great potential for the application in high-speed OFDM-based bandlimited VLC systems.

References

[1] T. Komine and M. Nakagawa, "Fundamental analysis for visible-light communication system using LED lights," *IEEE Trans. Consum. Electron.*, vol. 50, no. 1, pp. 100–107, Feb. 2004.

[2] I. Demirkol, D. Camps-Mur, J. Paradells, M. Combalia, W. Popoola, and H. Haas, "Powering the Internet of Things through light communication," *IEEE Commun. Mag.*, vol. 57, no. 6, pp. 107–113, Jun. 2019.

[3] C. Chen, S. Fu, X. Jian, M. Liu, X. Deng, and Z. Ding, "NOMA for energy-efficient LiFi-enabled bidirectional IoT communication," *IEEE Trans. Commun.*, vol. 69, no. 3, pp. 1693–1706, Mar. 2021.

[4] S. Rajagopal, R. Roberts, and S.-K. Lim, "IEEE 802.15.7 visible light communication: Modulation schemes and dimming support," *IEEE Commun. Mag.*, vol. 50, no. 3, pp. 72–82, Mar. 2012.

[5] J.-Y. Sung, C.-W. Chow, and C.-H. Yeh, "Is blue optical filter necessary in high speed phosphor-based white light LED visible light communications?" *Opt. Exp.*, vol. 22, no. 17, pp. 20646–20651, Aug. 2014.

[6] H. Le Minh *et al.*, "High-speed visible light communications using multiple-resonant equalization," *IEEE Photon. Technol. Lett.*, vol. 20, no. 14, pp. 1243–1245, Jul. 15, 2008.

[7] Y. F. Liu, Y. C. Chang, C. W. Chow, and C. H. Yeh, "Equalization and pre-distorted schemes for increasing data rate in in-door visible light communication system," in *Proc. Opt. Fiber Commun. Conf./Nat. Fiber Optic Eng. Conf.*, Mar. 2011, Paper JWA83, pp. 1–3.

[8] H. Elgala, R. Mesleh, and H. Haas, "Indoor broadcasting via white LEDs and OFDM," *IEEE Trans. Consum. Electron.*, vol. 55, no. 3, pp. 1127–1134, Aug. 2009.

[9] L. Zeng *et al.*, "High data rate multiple input multiple output (MIMO) optical wireless communications using white led lighting," *IEEE J. Sel. Areas Commun.*, vol. 27, no. 9, pp. 1654–1662, Dec. 2009.

[10] B. Lin, W. Ye, X. Tang, and Z. Ghassemlooy, "Experimental demonstration of bidirectional NOMA-OFDMA visible light communications," *Opt. Exp.*, vol. 25, no. 4, pp. 4348–4355, Feb. 2017.

[11] C. Chen, W.-De Zhong, H. Yang, and P. Du, "On the performance of MIMO-NOMA-based visible light communication systems," *IEEE Photon. Technol. Lett.*, vol. 30, no. 4, pp. 307–310, Feb. 15, 2018.

[12] S. Mardanikorani, X. Deng, and J.-P.-M. G. Linnartz, "Sub-carrier loading strategies for DCO-OFDM LED communication," *IEEE Trans. Commun.*, vol. 68, no. 2, pp. 1101–1117, Feb. 2020.

[13] H. Li, X. Chen, J. Guo, and H. Chen, "A 550 Mbit/s real-time visible light communication system based on phosphorescent white light LED for practical high-speed low-complexity application," *Opt. Exp.*, vol. 22, no. 22, pp. 27203–27213, 2014.

[14] Y. Wang, L. Tao, Y. Wang, and N. Chi, "High speed WDM VLC system based on multi-band CAP64 with weighted pre-equalization and modified CMMA based post-equalization," *IEEE Commun. Lett.*, vol. 18, no. 10, pp. 1719–1722, Oct. 2014.